3-19-2007

Plasmonic Materials in Transparency and Cloaking Problems: Mechanism, Robustness and Physical Insights

Andrea Alù
University of Pennsylvania

Nader Engheta
University of Pennsylvania, engheta@seas.upenn.edu

Postprint version. Published in *Optics Express*, Volume 15, Issue 6, March 2007, pages 3318-3332.
Publisher URL: http://www.opticsinfobase.org/abstract.cfm?URI=oe-15-6-3318

Plasmonic Materials in Transparency and Cloaking Problems: Mechanism, Robustness and Physical Insights

Abstract

The possibility of making a given object transparent to the impinging radiation, or cloaking it, by employing a suitable metamaterial or plasmonic cover has been recently studied theoretically, showing how this technique may overcome the limitations of other currently available techniques. Here we discuss the underlying mechanisms, physical insights and some computer simulations on the role of such homogeneous isotropic metamaterial covers near their plasma frequency in order to dramatically reduce the fields scattered by a given object. Not requiring any absorptive process, any anisotropy or inhomogeneity, and any interference cancellation, in this contribution we demonstrate, using full-wave numerical simulations, how a homogeneous isotropic plasmonic material shell may basically "re-route" the impinging field in such a way to make dielectric and even conducting or metallic objects of a certain size nearly transparent to an outside observer placed in its near as well as in its far field. In addition, it is discussed in detail how this technique, relying on a *non-resonant* phenomenon, is fairly robust to relatively high variations of the shape and of the geometrical and electromagnetic properties of the cloaked object.

Disciplines

Operations Research, Systems Engineering and Industrial Engineering

Comments

Postprint version. Published in *Optics Express*, Volume 15, Issue 6, March 2007, pages 3318-3332.
Publisher URL: http://www.opticsinfobase.org/abstract.cfm?URI=oe-15-6-3318

Plasmonic materials in transparency and cloaking problems: mechanism, robustness, and physical insights

Andrea Alù and Nader Engheta

University of Pennsylvania, Department of Electrical and Systems Engineering,
200 South 33rd Street, Philadelphia, PA 19104, U.S.A.
andreaal@ee.upenn.edu, engheta@ee.upenn.edu

Abstract: The possibility of making a given object transparent to the impinging radiation, or cloaking it, by employing a suitable metamaterial or plasmonic cover has been recently studied theoretically, showing how this technique may overcome the limitations of other currently available techniques. Here we discuss the underlying mechanisms, physical insights and some computer simulations on the role of such homogeneous isotropic metamaterial covers near their plasma frequency in order to dramatically reduce the fields scattered by a given object. Not requiring any absorptive process, any anisotropy or inhomogeneity, and any interference cancellation, in this contribution we demonstrate, using full-wave numerical simulations, how a homogeneous isotropic plasmonic material shell may basically "re-route" the impinging field in such a way to make dielectric and even conducting or metallic objects of a certain size nearly transparent to an outside observer placed in its near as well as in its far field. In addition, it is discussed in detail how this technique, relying on a *non-resonant* phenomenon, is fairly robust to relatively high variations of the shape and of the geometrical and electromagnetic properties of the cloaked object.

OCIS codes: (160.4670) Optical materials; (160.3900) Metals.

References and links

1. R. L. Fante, and M. T. McCornack, "Reflection properties of the Salisbury screen," IEEE Trans. Antennas Propag. **30**, 1443-1454 (1968).
2. J. Ward, "Towards invisible glass," Vacuum **22**, 369-375 (1972).
3. A. Alù, and N. Engheta, "Achieving transparency with plasmonic and metamaterial coatings," Phys. Rev. E **72**, 016623 (2005).
4. J. B. Pendry, D. Schurig, and D. R. Smith, "Controlling electromagnetic fields," Science **312**, 1780-1782 (2006).
5. D. Schurig, J. J. Mock, B. J. Justice, S. A. Cummer, J. B. Pendry, A. F. Starr, and D. R. Smith, "Metamaterial electromagnetic cloak at microwave frequencies," Science **314**, 977-980 (2006).
6. N. A. Nicorovici, R. C. McPhedran, and G. W. Milton, "Optical and dielectric properties of partially resonant composites," Phys. Rev. B **49**, 8479–8482 (1994).
7. G. W. Milton, and N. A. Nicorovici, "On the cloaking effects associated with anomalous localized resonance," Proc. R. Soc. Lond. A: Math. Phys. Sci. **462**, 3027–59 (2006).
8. U. Leonhardt, "Optical conformal mapping," Science **312**, 1777-1780 (2006).
9. L. Landau, and E. M. Lifschitz, Electrodynamics of Continuous Media (Pergamon Press, Oxford, UK, 1984).
10. R. W. Ziolkowski, and N. Engheta, (guest editors), IEEE Trans. Antennas Propag. **51**, 2546-2750 (2003).
11. W. Rotman, "Plasma simulation by artificial dielectrics and parallel-plate media," IRE Trans. Antennas Propag. **10**, 82-95 (1962).
12. J. B. Pendry, A. J. Holden, D. J. Robbins, and W. J. Stewart, "Low frequency plasmons in thin-wire structures," J. Phys. Condens. Matter **10**, 4785-4809 (1998).
13. J. A. Stratton, Electromagnetic Theory (McGraw-Hill Comp., New York and London, 1941).

14. C. F. Bohren, and D. R. Huffman, Absorption and Scattering of Light by Small Particles (Wiley, New York, 1983).
15. M. Kerker, "Invisible bodies," J. Opt. Soc. Am. **65**, 376-379 (1975).
16. CST Microwave StudioTM 5.0, CST of America, Inc., www.cst.com.
17. R. E. Collin, Field Theory of Guided Waves, (IEEE Press, New York, 1991).
18. A. Alù, A. Salandrino, and N. Engheta, "Negative effective permeability and left-handed materials at optical frequencies," Opt Express **14**, 1557-1567 (2006).

1. Introduction

Inducing transparency or low scattering by employing a suitable cover has been extensively studied by physics and engineering groups along the years, since it may have significant impact in various fields, e.g., optics, medicine, biology, and nanotechnology, to mention a few. Absorbers [Ref. 1] or anti-reflection coatings [Ref. 2] are common in some applications, but they show several limitations in the shape and material of the cloaked object, and in the inherent possibility of detecting their absorption or their interference patterns.

We see or detect objects by collecting the electromagnetic radiation that their surface/volume scatters when illuminated by a source. It is intuitive to think therefore that by covering an object with a passive non-absorptive material, consequently increasing its physical cross-section, one would also increase the scattered electromagnetic fields at a given frequency, making the object more detectible to an external observer, and this is generally the case. However, we have recently shown [Ref. 3] that when plasmonic materials or metamaterials (which can be homogeneous and isotropic), i.e., materials near their plasma frequency with an electric permittivity with low-positive or even negative value, are considered, the situation may differ substantially. In principle, in fact, it is possible to design a homogeneous, isotropic, passive non-absorptive (or low-loss) plasmonic cover in such a way that the scattering cross section of a given object of a certain electrical size is significantly reduced with respect to the case when the cover is not present, overcoming the aforementioned limitations of other techniques.

As shown in [Ref. 3], this may be explained by the fact that an object of dimensions smaller or comparable with the wavelength scatters a field dominated by its electric dipolar contribution, as the integral sum of its volume polarization. A material with low-positive or negative permittivity has a negative electric polarizability, since the local electric polarization vector $\mathbf{P} = (\varepsilon - \varepsilon_0)\mathbf{E}$ flips its sign when the material permittivity ε is less than that of the background material ε_0 (in the previous formula $\mathbf{E}$ is the local electric field inside the material). The presence of a plasmonic cover, therefore, basically acts as an "anti-phase" scatterer, inducing an oppositely-signed electric dipolar field that, if suitably designed, may cancel the one produced by the object, and thus providing a cloaking cover. If the cover has multiple degrees of freedom, for instance also an adjustable permeability, other multipole contributions might also be suitably canceled, obtaining a transparency effect also for larger objects that possess higher-order scattering terms.

Other different techniques to utilize metamaterials in order to reduce the scattering from a given obstacle have been recently presented in the technical literature [Ref. 4-8]. These techniques, however, rely on inhomogeneous and anisotropic metamaterials, with resonant inclusions, that need to be precisely designed for a given polarization and at a given band of frequency. Moreover, these setups so far considered in these examples are often idealized as 2D geometries.

Plasmonic materials, which are at the basis of the present manuscript, on the other hand, are available in nature at infrared (IR) and optical frequencies, since noble metals, polar dielectrics and some semiconductors show low-loss regions near their plasma frequencies [Ref. 9]. At microwaves and radio frequencies (RF), metamaterials [Ref. 10] with plasmonic features may be successfully synthesized, as it has been shown over the years [Ref. 10-12]. Moreover, this technique does not rely on any resonant process/inclusions, so it can be

reasonably fairly robust to changes in the geometrical or electromagnetic parameters of the involved objects, and may also exhibit certain robustness over a band of frequencies, as we discuss in Section 4.

In the following we summarize the theory underlying this anomalous scattering phenomenon and we present some full-wave computer simulations that may give physical insights into the roles of such metamaterial covers near their plasma resonance in order to reduce the fields scattered by a given object which results in a dramatic drop in its total scattering cross section. The mechanisms that allow a homogeneous isotropic plasmonic material shell to "re-direct" the impinging field in order to cloak dielectric and even conducting objects are extensively discussed. Full-wave simulations involving modifications of the shape/geometry of the object to be covered, the possible presence of material losses, material dispersion and frequency variation are also presented, showing how the *non-resonant* nature of this phenomenon makes it relatively robust to such changes and modifications of the original design.

2. Theoretical formulation

We had recently shown that a homogeneous, isotropic, spherical cover shell with outer radius a_c and permittivity ε_c is effective in cloaking a spherical object by canceling the electric dipolar scattering of the spherical object of radius a and permittivity ε, provided that the following dispersion equation is satisfied [Ref. 3]:

$$\begin{vmatrix} j_1(k\,a) & j_1(k_c a) & y_1(k_c a) & 0 \\ \left[k\,a\; j_1(k\,a)\right]'/\varepsilon & \left[k_c a\; j_1(k_c a)\right]'/\varepsilon_c & \left[k_c a\; y_1(k_c a)\right]'/\varepsilon_c & 0 \\ 0 & j_1(k_c a_c) & y_1(k_c a_c) & j_1(k_0 a_c) \\ 0 & \left[k_c a_c\; j_1(k_c a_c)\right]'/\varepsilon_c & \left[k_c a_c\; y_1(k_c a_c)\right]'/\varepsilon_c & \left[k_0 a_c\; j_1(k_0 a_c)\right]'/\varepsilon_0 \end{vmatrix} = 0, \quad (1)$$

with $k \equiv \omega\sqrt{\varepsilon\,\mu}$, $k_c \equiv \omega\sqrt{\varepsilon_c\,\mu_c}$ and $k_0 \equiv \omega\sqrt{\varepsilon_0\,\mu_0}$ (the wave numbers in the object, in the cover and in the background region), and $j_n(.)$, $y_n(.)$ are spherical Bessel functions [Ref. 13], and $[\;]'$ denotes differentiation with respect to the argument of the spherical Bessel functions. This is consistent with the analysis derived in [Ref. 3] for the generic multipole contribution to the scattering from a spherical object.

In the quasi-static limit, i.e., when the object is sufficiently small with respect to wavelength of operation, Eq. (1) reduces to the condition $a = \sqrt[3]{\dfrac{(\varepsilon_c-\varepsilon_0)[2\varepsilon_c+\varepsilon]}{(\varepsilon_c-\varepsilon)[2\varepsilon_c+\varepsilon_0]}}\,a_c$. The limit of impenetrable objects, which may be interesting in several applications at microwave and radio frequencies for conducting materials or at infrared and optical frequencies when the real part of permittivity has a sufficiently negative value, corresponds to $a = \sqrt[3]{(\varepsilon_0-\varepsilon_c)/(2\varepsilon_c+\varepsilon_0)}\,a_c$, condition achievable when plasmonic covers with $0 < \varepsilon_c < \varepsilon_0$ are employed. This is consistent with the quasi-static analysis reported in older works [Ref. 14-15], but for larger objects Eq. (1) should be applied.

When the scattering cross section (SCS) of the object to be cloaked is dominated by the electric dipole contribution, which is the case when its physical cross section is not large compared to the wavelength of operation, the choice of a cover satisfying Eq. (1) ensures the cancellation of its overall scattering due to the dominant dipolar term, making the object nearly transparent even to a near-field observer. This has been shown in [Ref. 3] for several numerical examples of dielectric spherical objects. Increasing the dimensions of the object, however, the number of multipolar terms contributing to its scattering rapidly increases, and

this is even more evident in the case of impenetrable objects, where the magnetic dipole contribution is generally non-negligible. The amount of scattering associated with each multipolar order from the given object is easily evaluated with a Mie expansion [Ref. 13]-[Ref. 14], since the different multipolar scattering orders are orthogonal to each other. In such cases, if condition (1) may be met by a suitably designed cover, the scattering portion associated with the electric dipole contribution is completely cancelled by the cover, whereas the other scattering orders remain generally unperturbed or modified in a minor way. New degrees of freedom in the cover design may be required, when necessary, to cancel simultaneously other multipolar orders, following a similar collective cancellation of the corresponding scattering contributions. For instance, in the following section we propose the case of an impenetrable sphere of dimensions comparable to the operating wavelength with electric and magnetic dipoles dominating its scattering. In such a case, the additional degree of freedom chosen to simultaneously cancel both scattering from electric and magnetic dipoles consists of utilizing a cover with magnetic as well as electric properties.

It is important to stress how this cancellation phenomenon does not rely on absorption or dissipation, nor on any inhomogeneity or anisotropy, nor on any other resonant phenomena (thus it is not highly sensitive to losses or to modifications of the object shape, nor requiring highly narrow frequency band of operation, as it is shown in detail in Section 4). Unlike the cases studied in [Ref. 4-8], here even with the presence of the *homogeneous isotropic* cover, the impinging wave is re-routed around the scattering object and re-directed to its back, giving the impression to the external observer as if the incident wave, independent of its wave front, were almost undisturbed, and thus the object were transparent. Under suitable conditions, this makes the covered object approximately transparent to an external observer, even if placed in the near-field. In the next sections we verify these predictions and give some insights into the mechanism underlying this phenomenon with some numerical simulations obtained using commercial finite-integration-technique (FIT) software [Ref. 16].

3. Numerical examples and physical insights

We consider here, as an example, the case of an impenetrable spherical object with diameter $2a = 0.4\lambda_0$ at the working frequency f_0 (in the following simulations the permittivity of the object is considered sufficiently negative in its real part or with a sufficiently high imaginary part to not allow wave propagation inside the object, which may model the case of a plasmonic material with high negative permittivity at infrared or optical frequencies or of a conductive metal at microwave frequencies). We have chosen the case of an impenetrable material to show more strikingly the effects of this "re-routing" of energy in the simulations when the suitable homogeneous isotropic cover is employed, since in this case no energy flow can cross the object, but these concepts apply also when dielectric or in general penetrable materials are considered, as we have already shown in [Ref. 3]. As already noted in the previous section, the impenetrable case is indeed the one where the presence of different multipolar scattering contributions is more evident even for relatively small objects. This makes the application of this cloaking phenomenon more challenging on the one hand and more exciting on the other.

Since the object size is comparable with the wavelength of operation, different orders contribute to its total SCS σ. The scattering orders have been evaluated in closed form by applying the Mie theory [Ref. 10-11], finding that for the case at hand $\sigma = 0.28\lambda_0^2$, dominated in particular by the electric and magnetic dipolar fields, contributing, respectively, to 77% and 20% of the total scattering (the residual 3% is represented by higher order multipolar scattering terms). A homogeneous isotropic cover designed following Eq. (1) to cancel the dominant electric dipolar contribution would have a shell radius $a_c = 1.09a$ with a permittivity $\varepsilon_c = 0.1\varepsilon_0$ at the frequency of interest. Using such a shell surrounding the impenetrable object may indeed be verified to suppress 79% of the total scattering cross section, reducing substantially the scattering of the object, but still leaving it detectable to an

external observer (notice how such a shell partially reduces also the contribution from higher scattering orders, reducing the scattering cross section of more than the electric dipole contribution only).

The magnetic dipole contribution would be mainly responsible for most of the residual scattering and in fact it may be verified that the near-field scattering in this case would be dramatically reduced in the H plane ($y-z$ plane in the following figures, with magnetic field parallel to this plane), but would remain substantially not modified in the E plane ($x-z$ plane in the following figures, with electric field parallel to this plane), where the contributions comes from the magnetic multipole moments. The plasmonic cover effectively acts as an 'anti-phase' scatterer, since the impenetrable sphere is polarized by the impinging field to radiate an electric dipole radiation in the H plane in phase with the impinging electric field, but the low-ε shell "cancels" this radiation due to its negative polarizability, as discussed above and in [Ref. 3]. This would be sufficient to make an object with small dimensions transparent, but in this case the residual scattering coming from higher-order contributions represents a non-negligible quantity.

In order to cancel this further contribution to the scattering, as already mentioned in the previous section, it is necessary to increase the degrees of freedom associated with the homogeneous isotropic cover design. Here we propose to utilize a material with magnetic as well as electric properties for the shell. It is interesting to note that since a small-sized impenetrable object has a negative magnetic polarizability [Ref. 17], this *cancellation* effect may be achieved by using just a material with permeability higher than that of free space (to produce a positive magnetic polarization in the surrounding shell). Magnetic materials with such values of permeability are available in nature at microwave frequencies. Magnetic effects in the inclusions of suitably designed metamaterials may give rise to the desired value at any frequency, even in the visible (see e.g., [Ref. 18]). The required permeability to obtain an optimized minimum value of the scattering, i.e., to cancel simultaneously both electric and magnetic dipolar contributions, may be furthermore tuned to the desired value by varying the low permittivity of the metamaterial cover. For instance, for a permittivity $\varepsilon = 0.1\varepsilon_0$ an optimum metamaterial shell has been numerically determined with $a_c = 1.15a$ and $\mu = 5.1\mu_0$. In this case, the total scattering cross section for the sphere is reduced to $\sigma = 2.22 \cdot 10^{-3} \lambda_0^2$, with a reduction of 99.2% of the total scattering cross section. In this case both planes of polarizations would see a dramatic reduction of the scattering both in the near and in the far field. The required material may be envisioned by embedding suitable inclusions [Ref. 11-12] in a magnetic host material with the required permeability, or by designing the inclusions to provide both electric and magnetic effects to work at the desired frequency [Ref. 10].

When larger objects are considered and the number of multipolar scattering orders increases, it may be possible to use multi-layer covers, employing optimization procedures for determining the set of parameters required to minimize the contribution from all the scattering orders. This is currently under investigation by our group. Indeed, the cancellation of one or two scattering orders, even when larger objects are considered, may still be performed with a homogeneous isotropic cover following the technique presented here.

We have performed extensive numerical simulations in order to study the mechanism and behavior of such a metamaterial shell around the metallic object. We have studied this phenomenon analytically with a Mie expansion technique and we have validated the results using commercial software employing a finite integration technique method (CST Microwave Studio™) [Ref. 16]. In these simulations we have considered realistic properties of such a metamaterial, i.e., dispersion with frequency, material losses and imperfections in the shape of the object and of the shell. As already outlined, since this cloaking mechanism does not rely on a resonance, the presence of such additional imperfections does not seem to weaken the use of our previous analysis and the results. In the following section, we consider more

thoroughly larger variations in the shape and the geometrical and electromagnetic parameters of the considered objects.

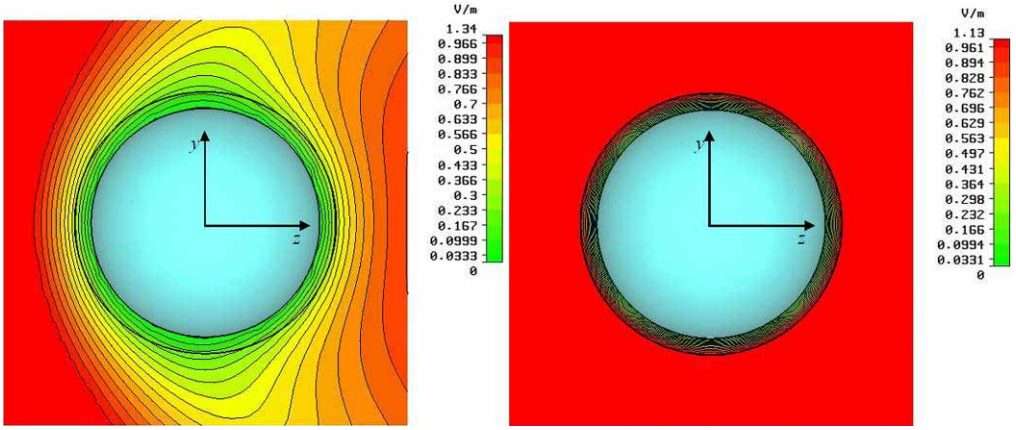

Fig. 1. (Left panel) Amplitude of the total electric field distribution in the H plane $x=0$ under plane wave excitation at $f=f_0$ for: an impenetrable sphere with diameter equal to $0.4\lambda_0$; (Right panel) the same sphere with the proper cloaking cover to reduce its scattering. The electric field is orthogonal to the plane of the figure.

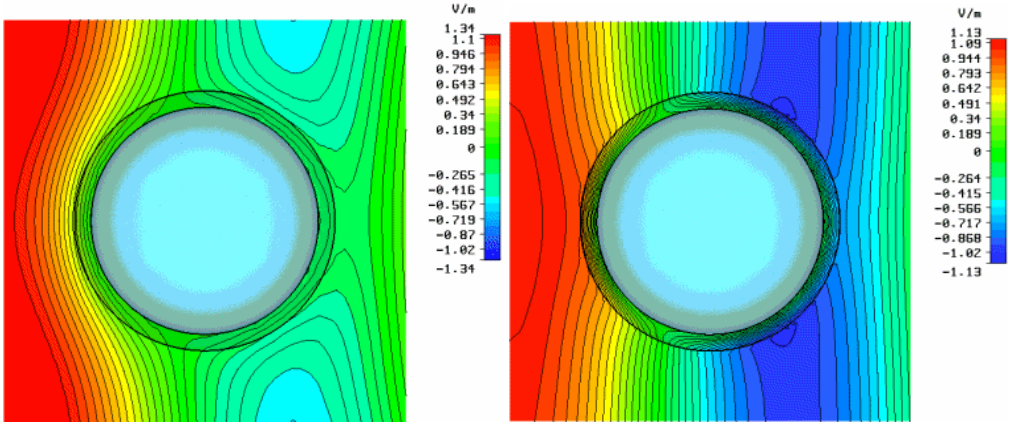

Fig. 2. Time-domain total electric field distribution in the H plane $x=0$ for the two cases of Fig. 1, i.e., on the left for an uncovered sphere (movie, 1.79 MB) and on the right for the covered sphere (movie, 1.91 MB). The electric field is orthogonal to the plane of the figure.

Note that in the present section all the figures refer to field plots calculated at the design frequency f_0 (next section will consider also the frequency dependence of this cloaking phenomenon). Figure 1 shows the total electric field amplitude distribution in the $x=0$ plane (H plane), under a plane wave excitation propagating along the z direction with a 1 V/m electric field linearly polarized along the x axis, in the two cases of the uncovered sphere (left panel) and the one with the metamaterial cover as the cloak, designed as described above, (right panel). For these numerical simulations, the cover has been designed including material losses and dispersion with frequency. A Drude model has been used to model the material properties, with $\varepsilon(f)=\left(1-f_p^2/\left[f\left(f-i\gamma\right)\right]\right)\varepsilon_0$, with $f_p=0.95\,f_0$ and $\gamma=0.016\,f_0$. In this way $\varepsilon(f_0)=(0.1+i0.015)\varepsilon_0$. Fig. 2 shows a movie of the total electric field in the time-domain plane wave propagation in the same plane for the two cases of uncovered and covered object under monochromatic excitation.

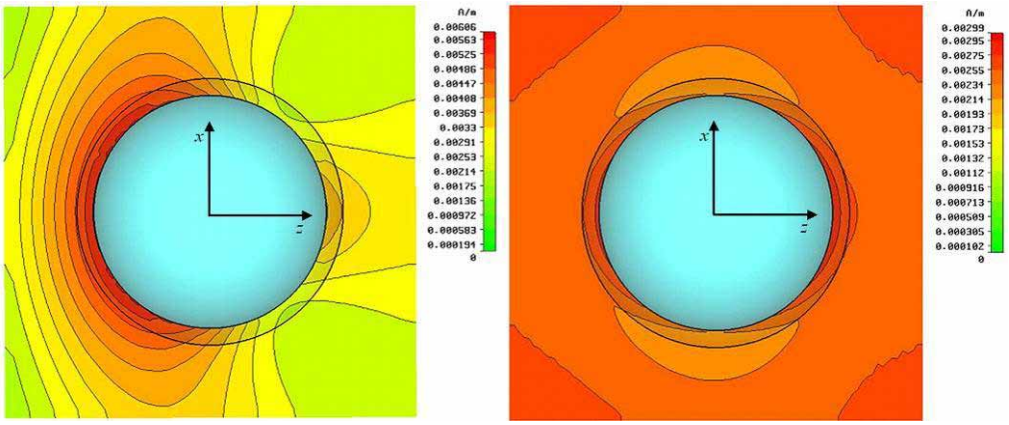

Fig. 3. Amplitude of the total magnetic field distribution in the E plane $y=0$ under plane wave excitation for the same cases as in Fig. 1. The magnetic field is orthogonal to the plane of the figure.

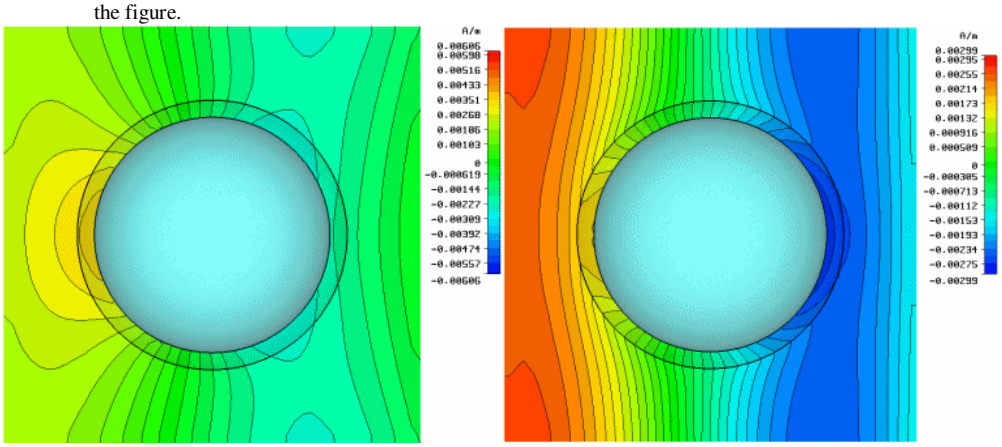

Fig. 4. Time-domain total magnetic field distribution in the E plane $y=0$ for the two cases of Fig. 2, i.e., on the left for an uncovered sphere (movie, 1.91 MB) and on the right for the covered sphere (movie, 2.21 MB). The magnetic field is orthogonal to the plane of the figure.

The magnetic field distribution in amplitude (Fig. 3) and in the time domain (Fig. 4), in the orthogonal E plane $y=0$ is also shown. These simulations clearly show how the cover drastically reduces the scattering of the object on both planes of polarization. The movies make also evident how the plane wave phase fronts are "restored" by the cover. It is clear from the figures how the cover approximately cancels the disturbance of the object in the region outside the cloaked object (but the field inside the cover is still affected), showing that the electromagnetic field outside the cover even in the near field is almost that of a plane wave propagating undisturbed. An external observer placed even very close to the cover surface, as well as in the far-field, would indeed not easily notice the presence of the cloaked object.

It is worth mentioning that by using just a homogeneous isotropic plasmonic material with low-positive permittivity and non-magnetic effects (which may be easier to produce, particularly at optical frequencies where plasmonic materials are present naturally, but magnetic effects are hard to be induced) the results of Fig. 1 and 2 in the E plane would remain substantially unchanged and the scattering in this polarization plane would remain very low and unmodified by the presence of magnetic properties in the cover. An increase in permeability is required to reduce the effects of the scattering from magnetic moments, which relate to Fig. 3 and 4 and contribute in this example to 20% of the total scattered power.

Figure 5 shows the power flow vector distributions in the two cases of uncovered and covered sphere in the H plane $x = 0$. Comparing the two plots it may be easily seen how the presence of the cover allows "re-routing" the power flow associated with the impinging radiation as if the covered object were almost transparent (even if the inner sphere is made of a highly conducting or highly plasmonic material, where no power flow can actually penetrate).

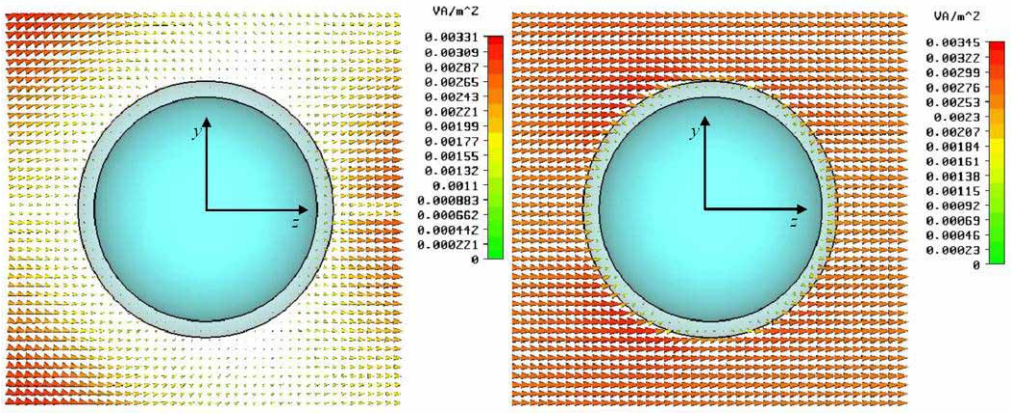

Fig. 5. Real part of the Poynting vector (power flow) distribution in the H plane $x = 0$ for the two cases of the uncovered (left) and covered (right) sphere.

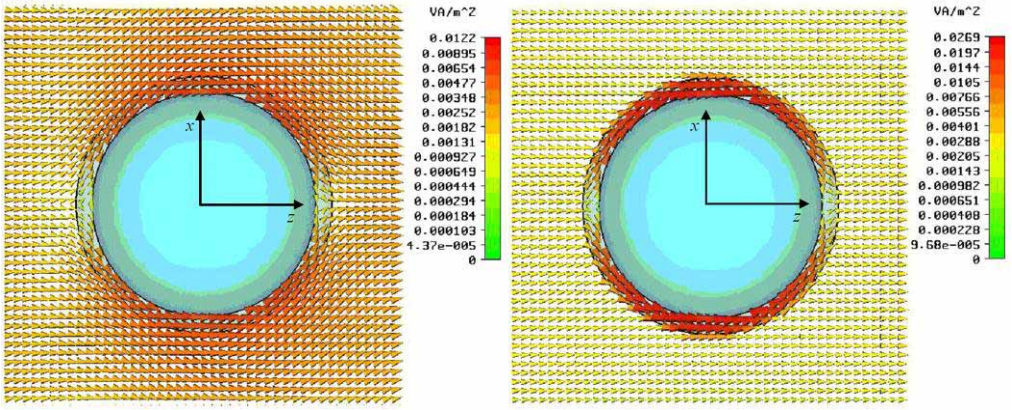

Fig. 6. Real part of the Poynting vector (power flow) distribution in the E plane $y = 0$ for the two cases of the uncovered (left) and covered (right) sphere.

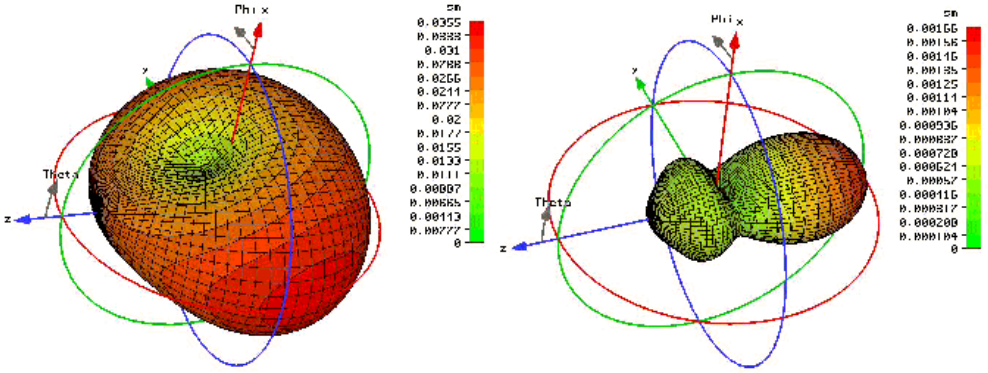

Fig. 7. 3-D scattering patterns for the two cases relative to the previous figures. Note that the two plots have two highly different scales.

In Fig. 6 it is reported the power flow in the orthogonal E plane $y = 0$, showing a similarly striking behavior when the cover is positioned around the impenetrable sphere. Both cases confirm that, when a suitable homogeneous isotropic cover is used, the power flow just outside the surface of the cover is substantially the same as the one of the impinging plane wave, undisturbed by the presence of the covered object. In particular, it is evident how in the E plane the tunneling of power through the cover, which is the main mechanism behind the cloaking phenomenon for such impenetrable objects, is more relevant.

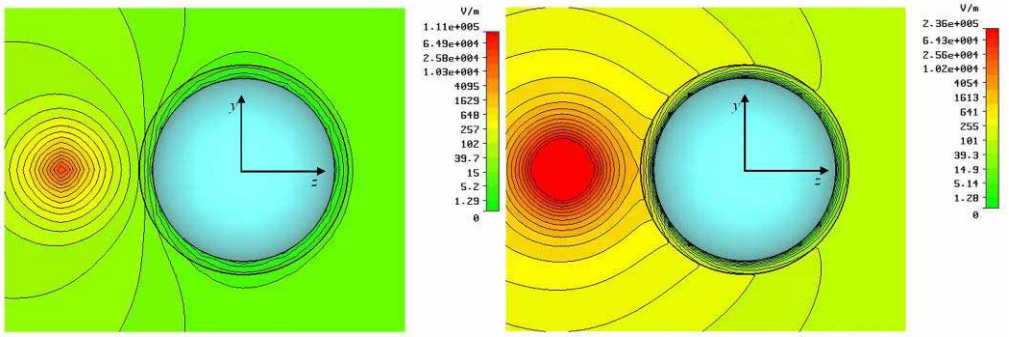

Fig. 8. Amplitude of the electric near-field distribution in the $x = 0$ H plane when an electric short dipole directed along x is placed in close proximity of the impenetrable object in the two cases of uncovered (left panel) and covered (right panel) sphere. The electric field is orthogonal to the plane of the figure.

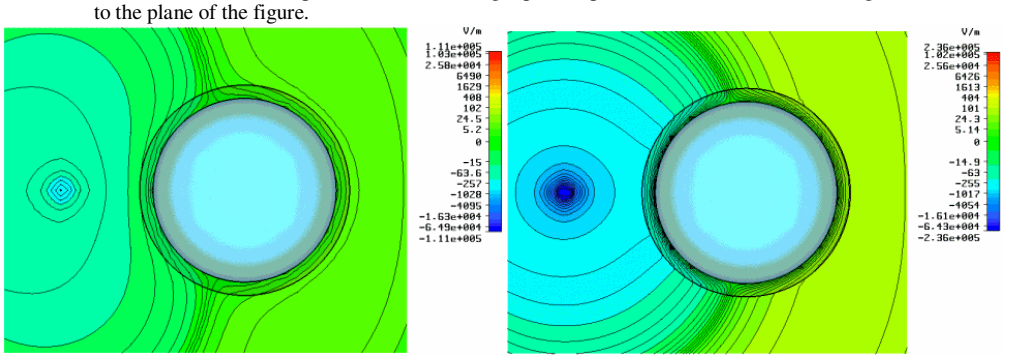

Fig. 9. Time-domain movies for the cases of Fig. 8: the uncovered case on the left (1.69 MB), the covered case on the right (2.16 MB). The electric field is orthogonal to the plane of the figure.

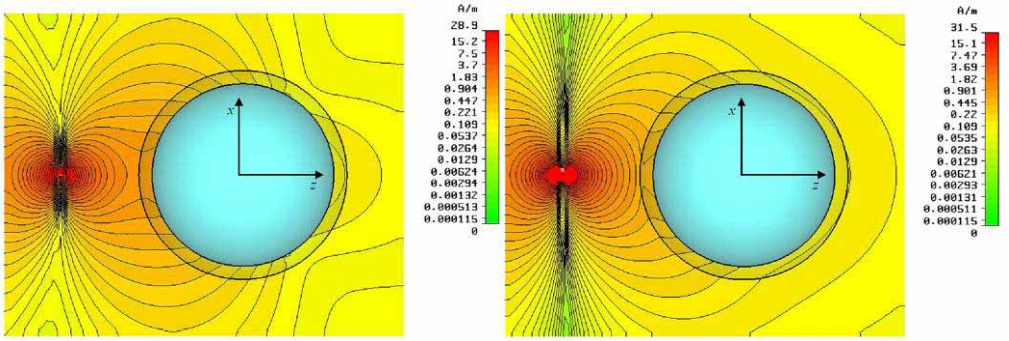

Fig. 10. Amplitude of the magnetic near-field distribution in the $y = 0$ plane when an electric short dipole directed along x is placed in close proximity of the impenetrable object in the two cases of uncovered and covered sphere. The magnetic field is orthogonal to the plane of the figure.

Figure 7 shows the far-field scattering patterns in the two cases of uncovered and covered spheres, showing the drastic reduction in the far-field SCS due to the presence of the cover (notice that the two plots have two very different scales). This confirms that the cover is effective in cloaking the object in the far as well as in the near field and in all directions.

As a final simulation for this section, we have placed a short electric dipole antenna near the impenetrable object with and without the metamaterial cover. Fig. 8 shows the electric near field distribution on the $x=0$ plane when a short electric dipole directed along x is placed in close proximity of the object (in this example it is at $\lambda_0/5$ from the surface of the impenetrable sphere). It is surprising how the spherical wave fronts of the dipolar radiation patterns are restored right outside the covered object when the homogeneous isotropic cover is applied. An observer placed behind the sphere may clearly notice the presence of the dipole as if almost the impenetrable sphere effectively were not there, even though the radiation cannot cross the metallic object. This confirms the prediction that the presence of the cover effectively allows a re-routing of the wave impinging on it, independent of the specific shape of its wave fronts, and even for a source placed in its near-field. An observer behind the object can "see" what is present on the other side of the object, even in this case for which the object itself does not allow the energy to pass through it, thanks to the anomalous tunneling/re-routing properties of the cloaking shell. Fig. 9 shows this effect in the time domain as a movie for the cases of uncovered and covered spheres, whereas the magnetic distribution on the E plane $y=0$ is given as the amplitude in Fig. 10 and as a time-domain movie in Fig. 11.

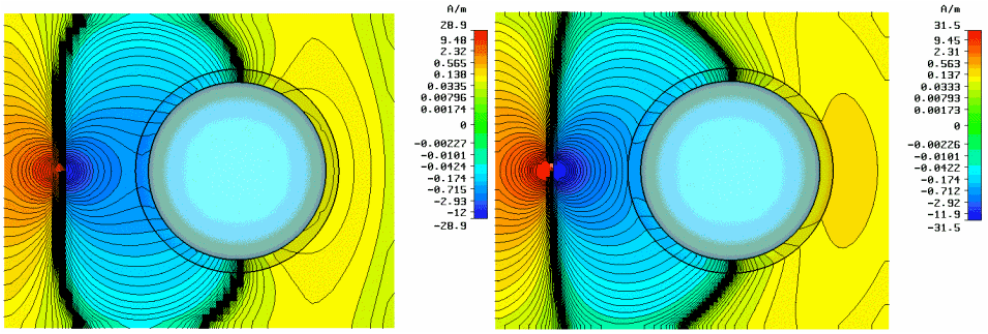

Fig. 11. Time-domain movies for the cases of Fig. 10: the uncovered case on the left (1.69 MB), the covered case on the right (2.16 MB). The magnetic field is orthogonal to the plane of the figure.

4. Robustness to geometry/shape/frequency variations and material losses

As claimed in the previous sections, the main physical phenomenon described in this manuscript does not rely on a material resonance and therefore it is not severely limited by strict conditions on the geometrical shape of the objects involved, or by the strict design of the frequency of operation and/or the electromagnetic parameters. Its robustness to geometrical variations due to fabrication processes and/or the presence of material losses is therefore expected to be relatively high.

In this section we demonstrate these assertions with full-wave simulations of more complex scenarios, in which shape variations and/or material losses come into play. Fig. 12, as a first example, reports the simulated results for the geometry analyzed in the previous section when symmetric cuts are applied along the three different axes, as depicted in the insets of the figure. In particular, the plot reports the maximum in the SCS (normalized to the square of operating wavelength, λ_0^2), varying the frequency of operation. The modified geometry has been obtained by applying cuts to the original spherical object in such a way that the bases of the cut away spherical caps have a radius that is half of the object radius. The consequent modification in shape of the cloaked object, therefore, is pretty drastic, and it may indeed represent possible imperfections in the realization process or unwanted variations in the object shape. The cover design has been kept the same as in the previous section, i.e.,

optimized for the ideal spherical shape of the inside object, and the cover material, following the same Drude model dispersion applied in the previous section, fills the space left empty by the cap removal. It can be seen from these plots that, despite the drastic difference in the object to be hidden, the phenomenon described here maintains its interesting properties: in the neighborhood of the design frequency f_0 the cross section of the object is drastically lowered, fairly independent of the location of the cuts. The lines representing the uncloaked cases are shown as dashed lines, with the same color legend. Moreover, the uncut (and uncloaked) case is also reported with the dashed green line. It is evident how the cloaking phenomenon is essentially unaffected by the modification in shape of the inner object.

As an aside, Fig. 12 also provides some insights into the frequency dependence of the cloaking phenomenon described in this manuscript. It is evident how the unusually low scattering is not just at one single specific frequency (or over a very narrow band), as it would happen in a resonant phenomenon, but instead the scattering goes down smoothly with frequency around the design frequency, and a drastic reduction of scattering is expected for a reasonably wider frequency range. As evident from this figure, a drastic reduction of the SCS with respect to the uncovered case is expected over a 10% fractional bandwidth.

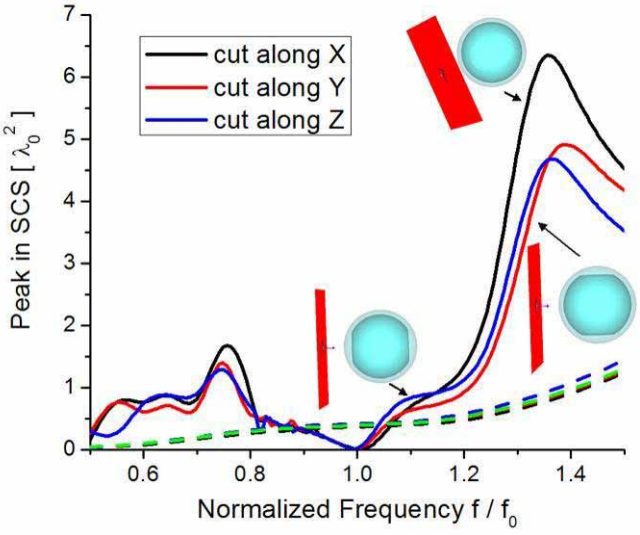

Fig. 12. Normalized peak in the scattering cross section for the sphere analyzed in Section 3 with symmetrical cuts in its left and right (black line), top and bottom (red) and front and back (blue), as also indicated by the insets. The dashed lines correspond to the cases in which the corresponding spheres are not cloaked by the metamaterial cover. The dashed green line corresponds to the uncut and uncloaked sphere.

Figure 13 reports the movie of the time-domain plane wave propagation (electric field distribution) in the H plane for the three different cases at the design frequency f_0. Again, we can see that, despite the relatively strong modification of the object shape, the plane wave impinging on the object to be cloaked is almost unperturbed by the covered object, even when the cuts are in the same directions as the polarizing electric field, which one may expect to be the more challenging case, implying the robustness of this cloaking phenomenon (Fig. 13 left, corresponding to the black line in Fig. 12).

Figure 14 reports the real part of the Poynting vector distribution in the three different cases and on both H and E planes, showing how the rerouting phenomenon is still preserved, despite the drastic variation in the geometry of the covered object. Again, it is in the E plane that the re-routing and tunneling phenomenon mainly takes place.

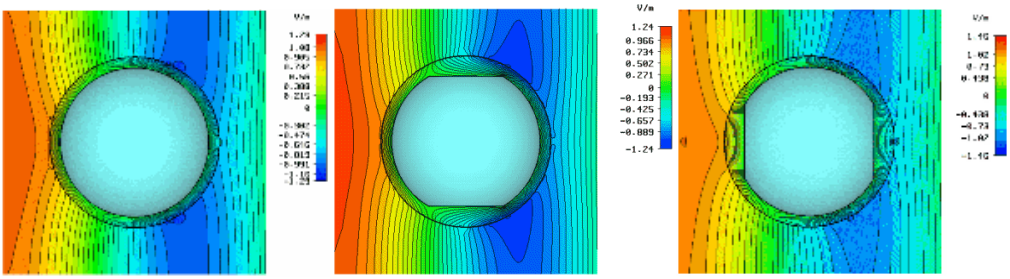

Fig. 13. Time-domain total electric field distribution in the H plane $x = 0$ for the three cases relative to the covered sphere of Section 3, but applying two symmetrical cuts in the direction of the impinging electric field (left, movie, 2.47 MB), in the direction of the impinging magnetic field (middle, movie, 2.27 MB), and in the direction of propagation of the impinging plane wave (right, movie, 2.25 MB).

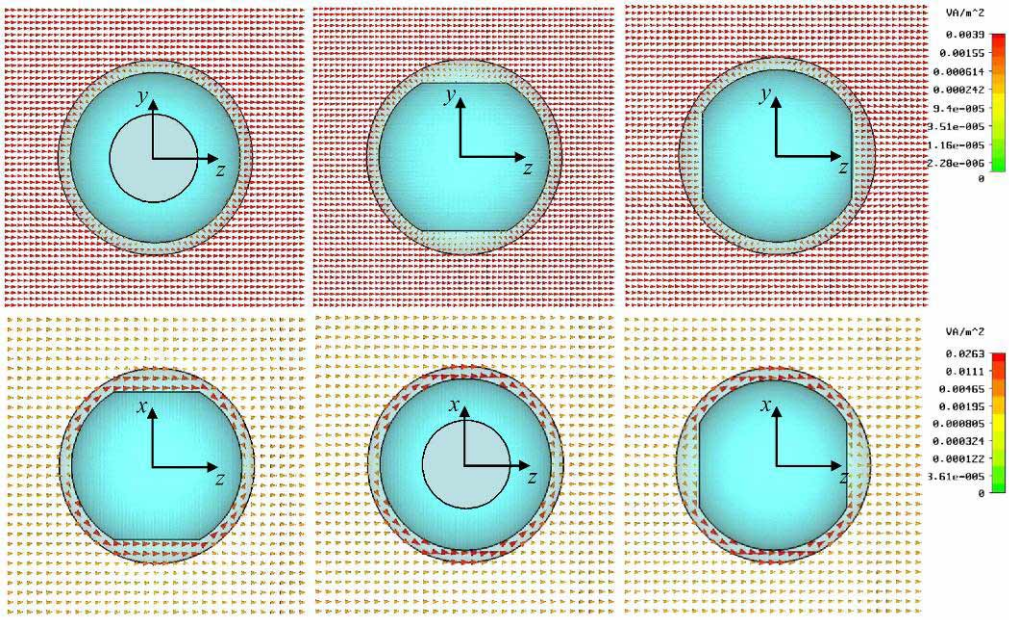

Fig. 14. Real part of the Poynting vector (power flow) distribution in the H plane $x = 0$ (top row) and E plane $y = 0$ (bottom row) for the three cases of Fig. 13.

Figure 15, as a further quantitative discussion on the robustness of this setup, shows a contour plot for the case of original sphere simulated in Section 3, showing the variation of the total SCS (evaluated analytically with a Mie expansion) versus both the ratio a_c / a and the frequency of operation f / f_0, still assuming a Drude model as in the previous section. Darker regions in the plot correspond to lower SCS. The other design parameters are kept the same as in the previous section. It is evident from the figure how the region of cloaking is not limited to a single point in the plot, i.e, for a single frequency and geometry, but instead it has a fairly and reasonably wider extension, with a maximum bandwidth located around the numerically optimized value $a_c = 1.15a$ employed in the previous section. Even for negative values of permittivity, as shown in [Ref. 3], the cloaking phenomenon is possible, which corresponds in the plot to $f < f_0$, and this explains the dark region in the bottom of the plot where again the SCS goes to zero. These results again confirm the flexibility of this cloaking technique.

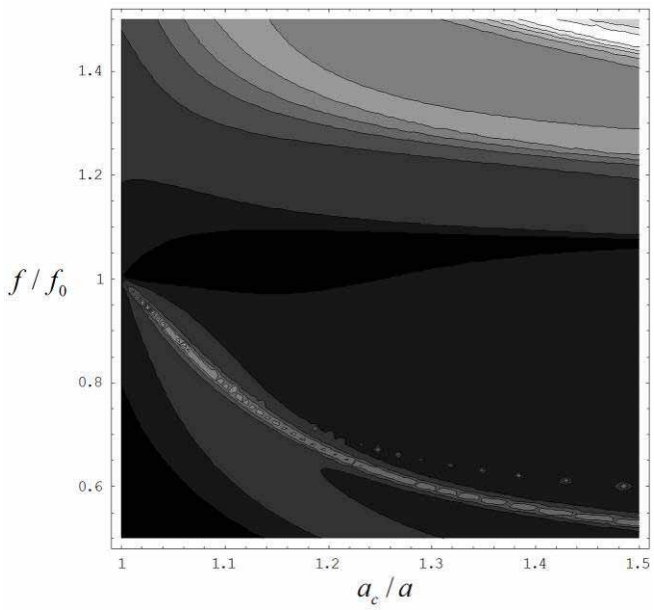

Fig. 15. Contour plot of the total SCS for the sphere simulated in Section 3, varying the frequency of operation and the ratio of radii a_c / a. Darker regions correspond to lower values of the total SCS.

Fig. 16, as a further example, shows the variation of the maximum peak in scattering cross section versus frequency, when changing the loss factor in the Drude model used in the previous section, i.e., varying the ratio γ / f_p. It is evident how, even for relatively high losses, higher than realistic losses in several examples of noble metals and polar dielectrics at infrared and optical frequencies and in metamaterials at lower frequencies, the transparency and cloaking phenomenon is still present around the design frequency f_0. In the extreme case $\gamma = f_p$, the wave does not penetrate the cover at all, due to the high material absorption, and therefore this case does not allow the predicted scattering reduction. For comparison, the dashed green line reported in the plot refers to the uncovered sphere. From analyzing these plots, it is clear that already at a level of $\gamma = 0.1 f_p$ the scattering reduction is present, and for even lower values of losses the SCS of the object is practically near zero. This further example confirms the robustness of this setup and the feasibility of this cloaking phenomenon.

As a final example in demonstrating the robustness of this phenomenon to shape variations of the cloaked objects and/or possible technological imperfections, Fig. 17 reports the peak in the normalized SCS as a function of the operating frequency for the example studied in Section 3, but adding several small imperfections (i.e., "roughness") on the surface of the metallic sphere. In particular, such imperfections are in the form of small hemispheres that are either added ("bumps") or carved ("dimples") to the spherical surface of the object. The radius of such hemispherical imperfections is 1/20 of the sphere's radius. As evident, their presence does not influence sensibly the previous results and the cloaking phenomenon remains mainly unaffected. Fig. 18 reports time-domain simulations (movie) of the two cases of Fig. 17, i.e., the covered spheres with bumps (left) and dimples (right) in the H plane, showing again the reconstruction of the wave fronts produced by the cloaking shell, despite the imperfections in the cloaked object.

5. Conclusions

In this contribution we have reviewed how the use of homogeneous isotropic plasmonic and metamaterial covers may drastically reduce the scattered field from 3D impenetrable objects

of dimensions comparable with the wavelength, effectively providing a cloaking technique. We have provided full-wave simulations and animations of the mechanism underlying this cloaking effect when a conducting or highly plasmonic object is to be cloaked. The results reported clearly show how the "anti-phase" scattering properties of properly designed plasmonic covers may be effective in making transparent conducting, plasmonic, as well as dielectric objects [Ref. 3] of dimensions comparable with the operating wavelength. Compared to recently presented alternative cloaking methods, this technique relies on metamaterials with homogenous and isotropic properties and it can be easily applied to fully 3D objects.

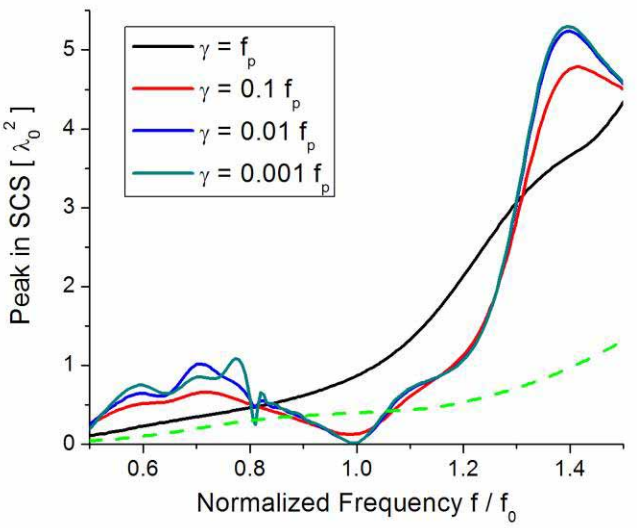

Fig. 16. Normalized peak in the SCS for the sphere analyzed in Section 3 when the level of losses is varied in the Drude model for the material of the cover. The dashed green line corresponds to the uncloaked sphere.

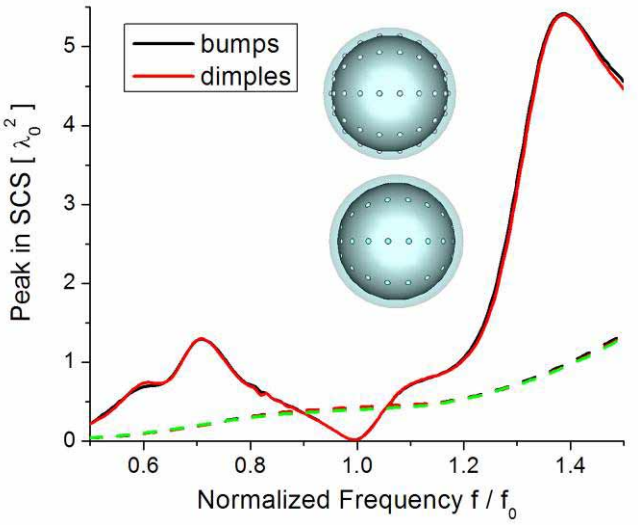

Fig. 17. Normalized peak in the SCS for the sphere analyzed in Section 3 when small imperfections (roughness) are added as "bumps" or carved as "dimples" in the metallic spherical surface. The black and red dashed lines refer to the cases where the corresponding spheres are uncovered. The dashed green line corresponds to the uncovered original sphere with no bumps or dimples.

We have also shown with different numerical examples how the sensitivity to the geometrical parameters, shape, frequency or presence of losses is relatively weak in this scheme, since it does not rely on any resonant effect. This can be a clear advantage in practical situations. In our opinion, this effect may open doors to exciting new applications in various fields.

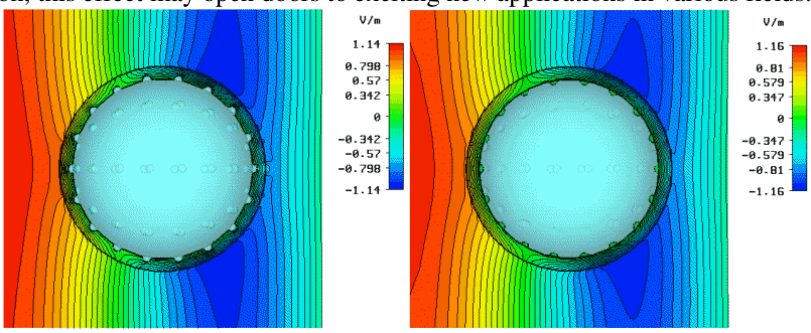

Fig. 18. Time-domain (movie) total electric field distribution in the H plane $x = 0$ for the two cases of Fig. 17, i.e., on the left for a cloaked sphere with bumps (movie, 2.41 MB) and on the right for the cloaked sphere with holes (movie, 2.41 MB). The electric field is orthogonal to the plane of the figure.

Acknowledgments

Correspondence should be addressed to Nader Engheta, by phone: 215-898-9777; fax: 215-573-2068; or e-mail: engheta@ee.upenn.edu.